Electronic Supplementary Material (ESI) for Physical Chemistry Chemical Physics.

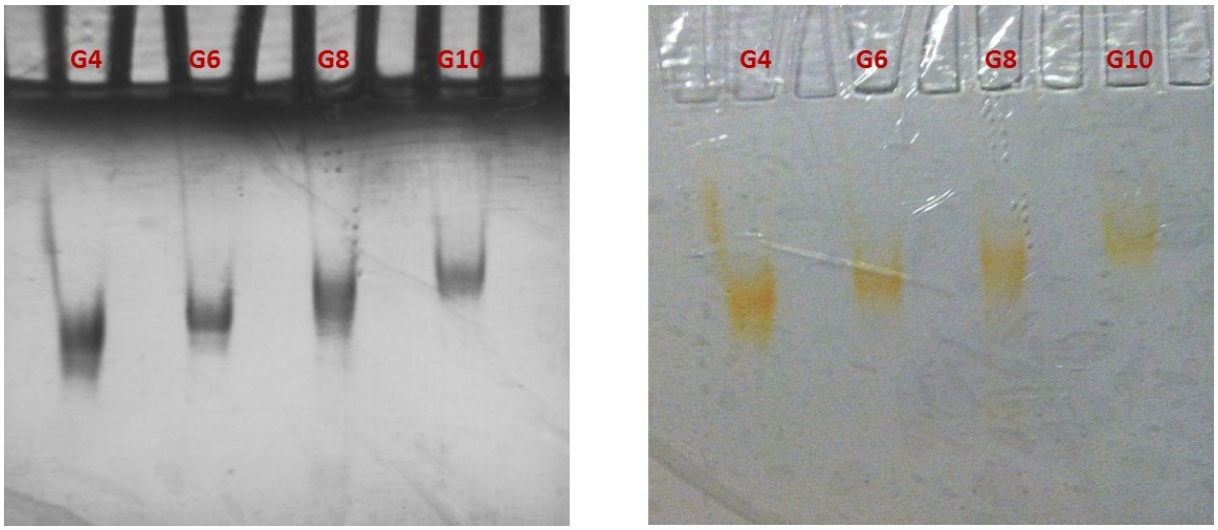

Figure S1: (Left) UV shadow cast against a TLC plate of native polyacrylamide gels of $d(T_4G_nT_4)_4$ oligonucleotides containing bound CuTMpyP4, where from left to right lanes are ordered from lower to higher molecular weights (see text above lanes for specific sequence). 100 μmol L^{-1} strand concentration of gel-purified oligonucleotide in 10 mmol L^{-1} KP_i, 50 mmol L^{-1} KCl at pH 7.0. (Right) Visible image of the same gel.

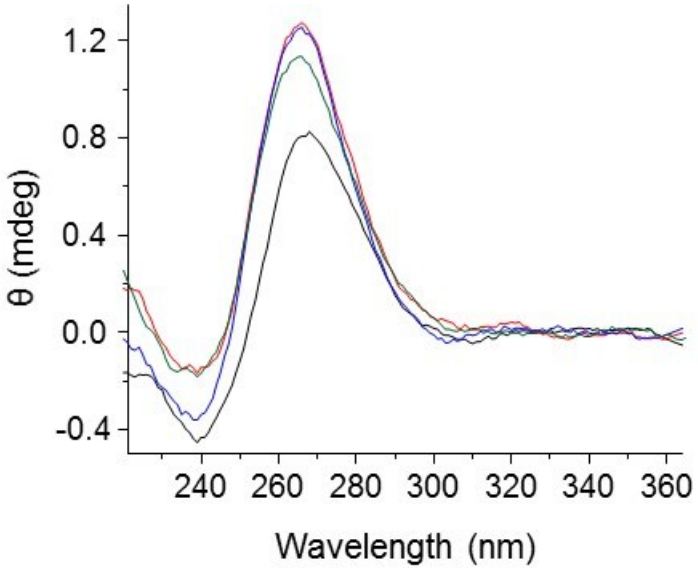

Figure S2: Representative circular dichroism spectra. (black) G4 + CuTMPyP4; (green) G6 + CuTMpyP4; (red) G8 + CuTMPyP4; (blue) G10+ CuTMPyP4. Solutions for CD experiments in 10 mmol L^{-1} potassium phosphate with 50 mmol L^{-1} KCl contained gel-purified G4, G6, G8 and G10, with bound CuTMpyP4 at concentrations of 37.6 μmol L^{-1}, 31.6 μmol L^{-1}, 40.0 μmol L^{-1} and 38.6 μmol L^{-1}, respectively, at a matched oligonucleotide optical density of 4.0.

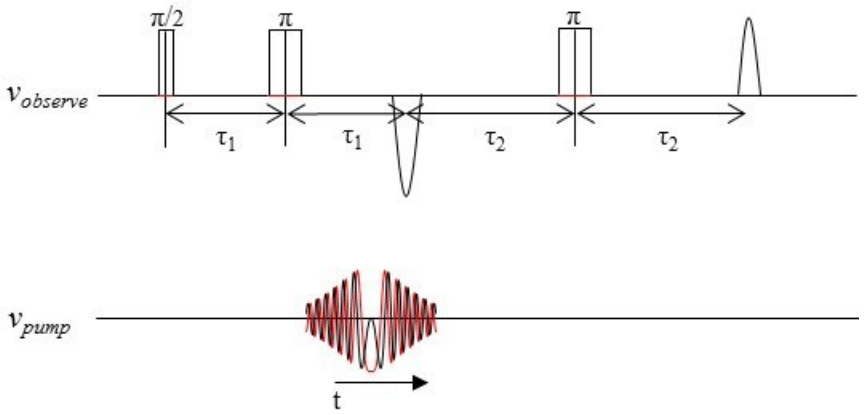

Figure S3: The four pulse double electron electron resonance (DEER) sequence showing the X component (black) and Y (red) components of the pulses. A refocused echo is generated at time $= 2\tau_1 + 2\tau_2$ using conventional rectangular pulses at the observer frequency, and is modulated with the electron-electron dipolar coupling by an inversion pulse at the pump frequency. A sech/tanh pulse is generated at the pump frequency. See the main text for timings.

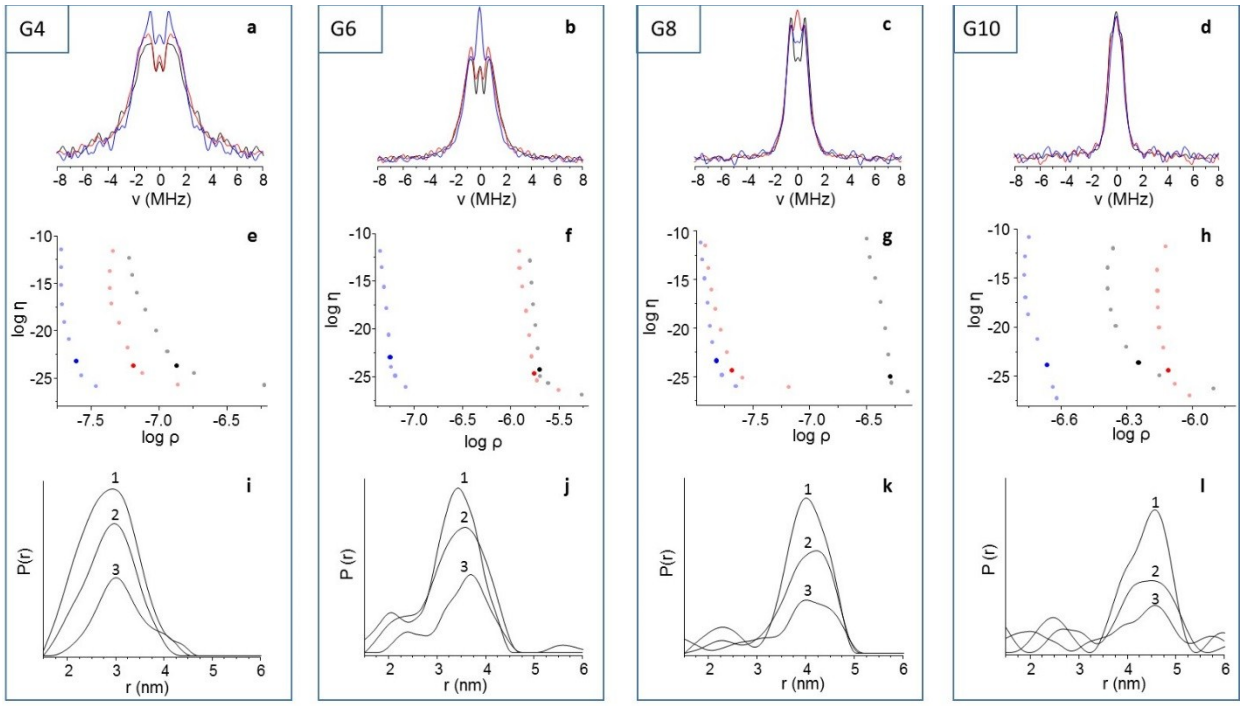

Figure S4: Analysis and extraction of distance distributions using Tikhonov regularization. Data sets are columnated according to quadruplex length, which is specified in the upper left corner of each column. (**a**-**d**) The Pake patterns for each measurement. The black traces correspond to field position 1, the red traces correspond to field position 2 and the blue traces correspond to field position 3 indicated in Figure 2. (**e**-**h**) L-curves, the solid circle indicates the chosen regularization parameter, with the same color code convention as in panels **a**-**d**. (**i**-**l**) The distance distributions extracted from fits to the form factors.

The distance distributions extracted using Tikhonov regularization of G6 + CuTMpyP4, G8 + CuTMpyP4 and G10 + CuTMpyP4 all contain ghost peaks at approximately 2.3 nm. These could possibly arise from nuclear modulation effects, and have been observed in DEER distance distributions of Mn^{2+} terpyridine complexes[1]. A two-pulse ESEEM time trace displaying nuclear modulations on the echo decay, the potential source of the observed short distances, is in Figure S9. Control experiments performed on the position of the pump pulse and also its shape were performed on G8 + CuTMpyP4 and are shown in Figure S9. These experiments revealed similar distributions, ruling out the possibility of artifacts arising from either orientation selection or overlap of the observer and pump excitation bands.

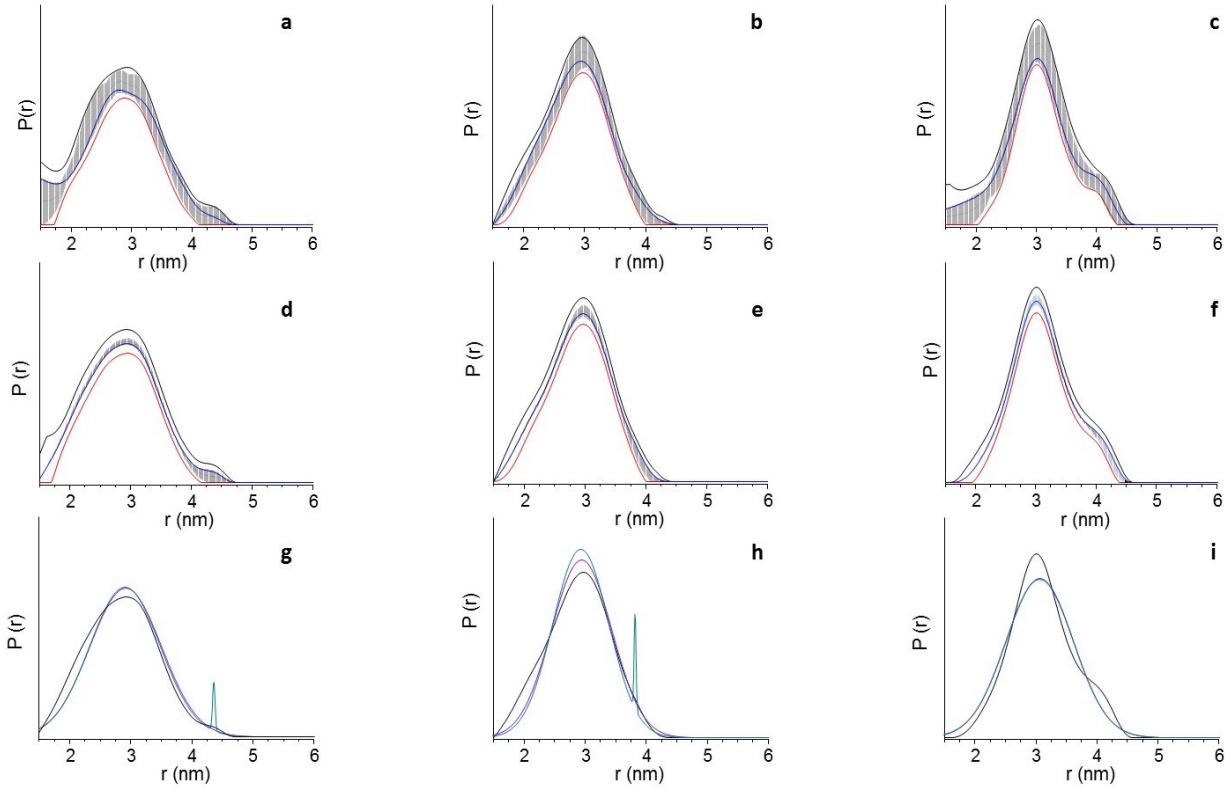

Figure S5: Error analysis of the uncertainty in the background correction to the DEER time trace of G4 + CuTMpyP4 used in Tikhonov regularization, and distance distribution comparison to model fitting. **(a-c)** The starting time for the background fitting is varied from t = 240 ns to t = 2000 ns over a total of 11 trials for field positions **1**, **2** and **3** on Figure 2, respectively. The influence of noise is concomitantly tested through artificial enhancement by adding pseudorandom numbers so that the noise level is increased by a factor of 1.5. **(d-f)** Only the starting time is varied at field positions **1**, **2** and **3** on Figure 2, respectively. For Figures **(a-f)**, the red line displays a lower error estimate corresponding to the mean value of the probability minus two times its standard deviation, the black line displays an upper error estimate corresponding to the mean value of the probability plus two times its standard deviation, and the blue line represents the distance distribution with the best root mean square deviation. Grey error bars indicate the full variation of the probability over all trials. All Figures **a-f** were analyzed at the optimum α parameter on the L-curve (see Figure 3). **(g-i)** Comparison of the mean distance distribution extracted from the error validation of Tikhonov regularization (black line) to the raw data fitted without *a priori* background correction using one (violet line) and two (teal line) Gaussian peaks. Distributions extracted using both methods have been normalized. (Tri-modal Gaussian distributions are omitted for clarity).

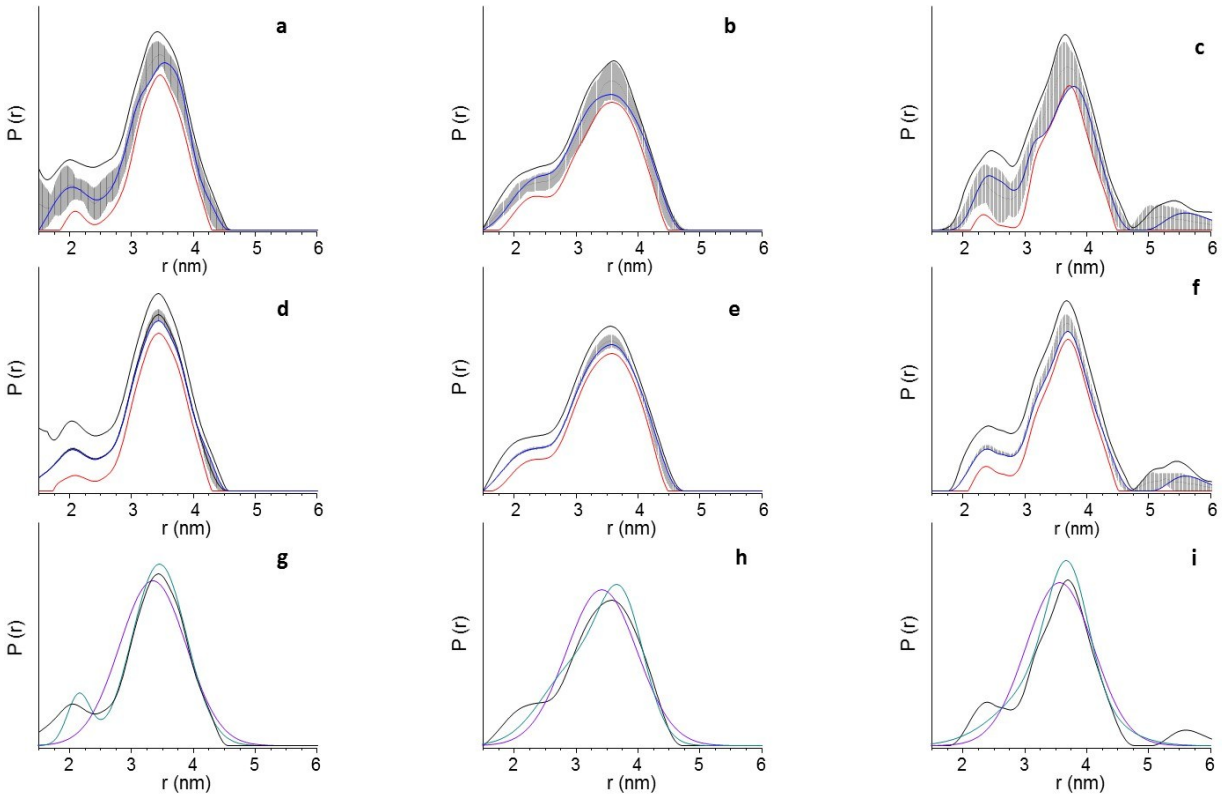

Figure S6: Error analysis of the uncertainty in the background correction to the DEER time trace of G6 + CuTMpyP4 used in Tikhonov regularization, and distance distribution comparison to model fitting. Panels **a-i** carry the same descriptors as for Figure S5.

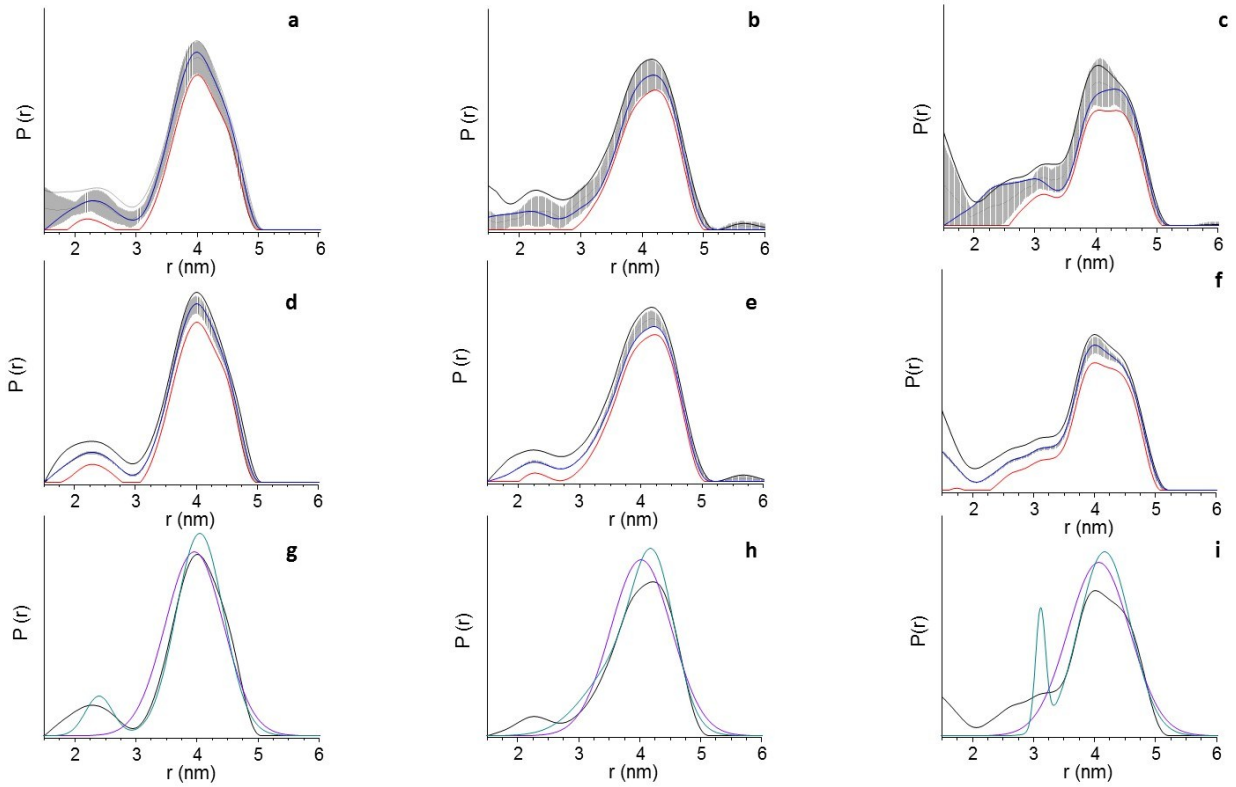

Figure S7: Error analysis of the uncertainty in the background correction to the DEER time trace of G8 + CuTMpyP4 used in Tikhonov regularization, and distance distribution comparison to model fitting. Panels **a-i** carry the same descriptors as for Figure S5.

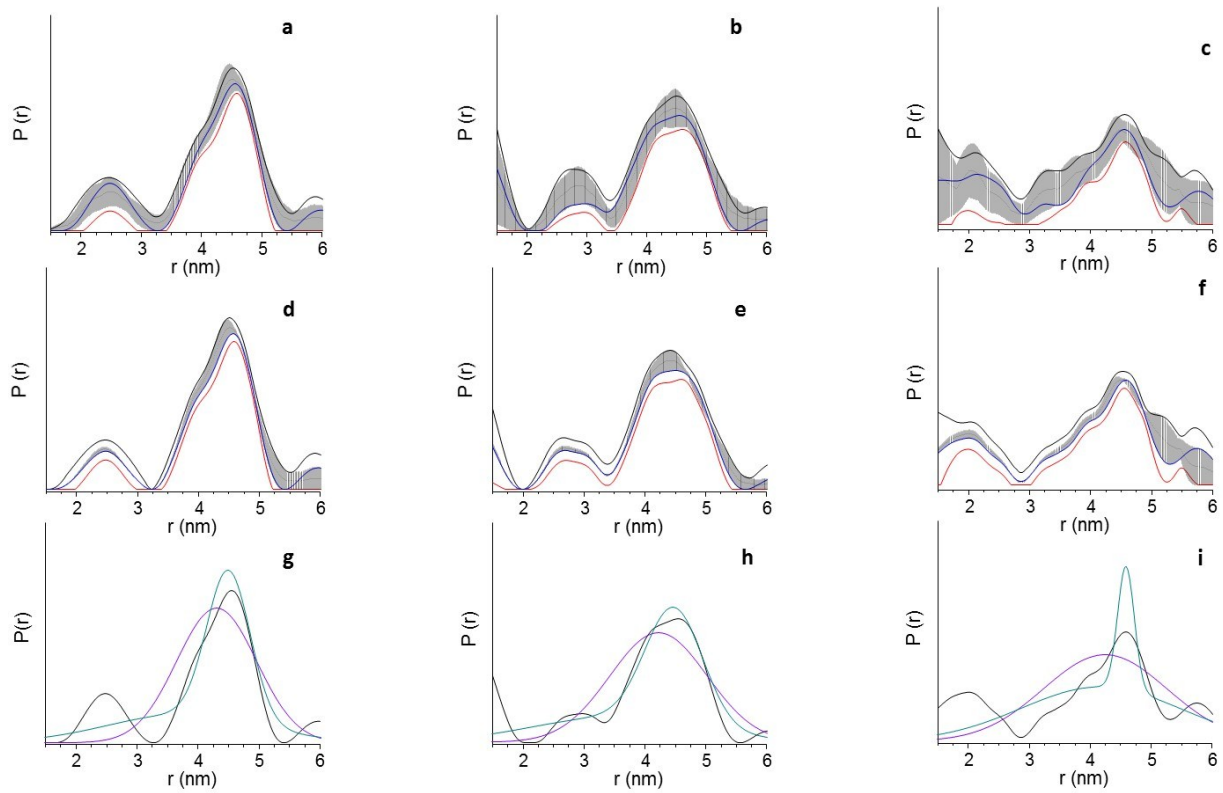

Figure S8: Error analysis of the uncertainty in the background correction to the DEER time trace of G10 + CuTMpyP4 used in Tikhonov regularization, and distance distribution comparison to model fitting. Panels **a-i** carry the same descriptors as for Figure S5.

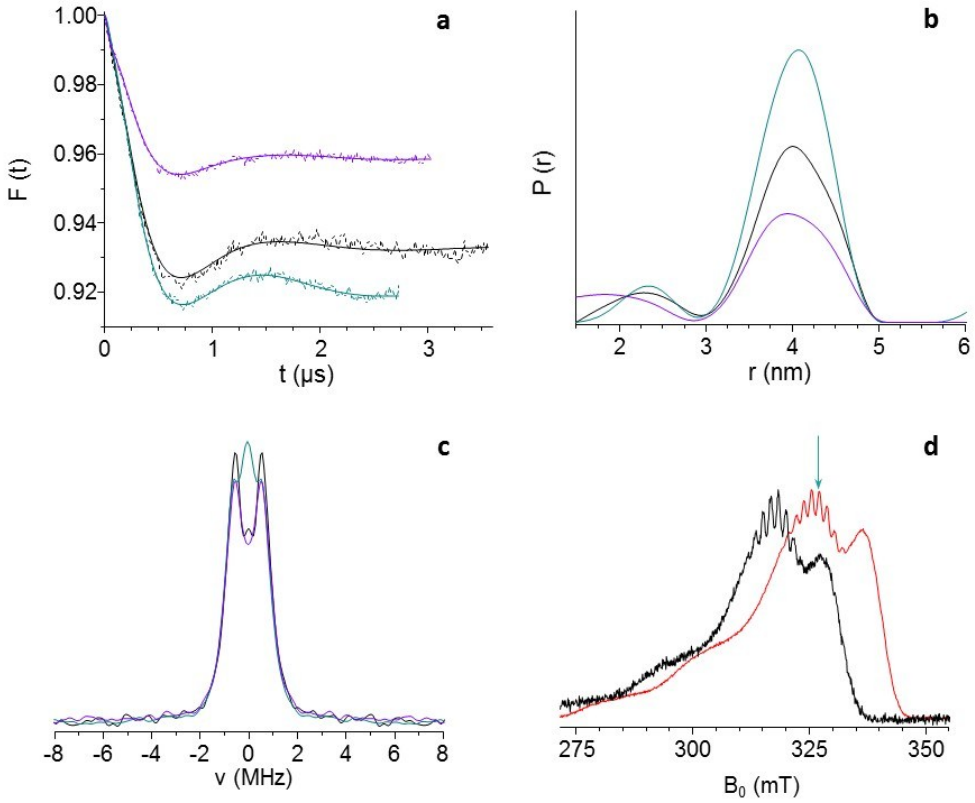

Figure S9: Comparison of signals using G8 + CuTMpyP4 with alternative ν_{offset} and pump pulse shape. **(a-c)** Background subtracted DEER trace, distance distribution using Tikhonov regularization, and FFT of time domain signal. Black traces: G8 + CuTMpyP4 at field position **1** in Figure 2 using ν_{offset} = 135 MHz and a 200 ns sech/tanh pump pulse. Violet traces: the same spectral parameters as the black traces, but with a 26 ns rectangular pump pulse. Teal traces: the same spectral parameters as the black traces, but with ν_{offset} = -252 MHz. **d** Field swept echo detected EPR spectra at the pump (red) and observer (black) frequencies with ν_{offset} = -252 MHz, where the arrow indicates the field position.

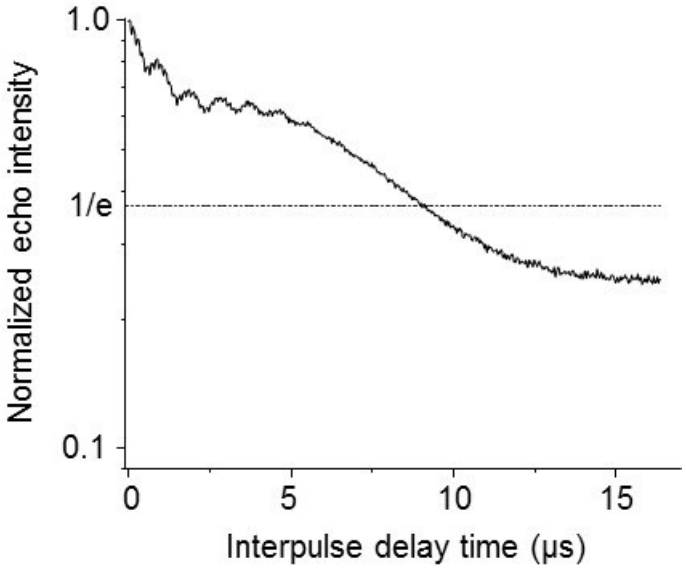

Figure S10: Hahn-echo decay of G8 + CuTMPyP4 as a function of the interpulse delay time. The field was set to position **1** at the pump frequency. The temperature was 30 K, the pulses were 16 ns and 32 ns, and the initial interpulse delay was 400 ns.

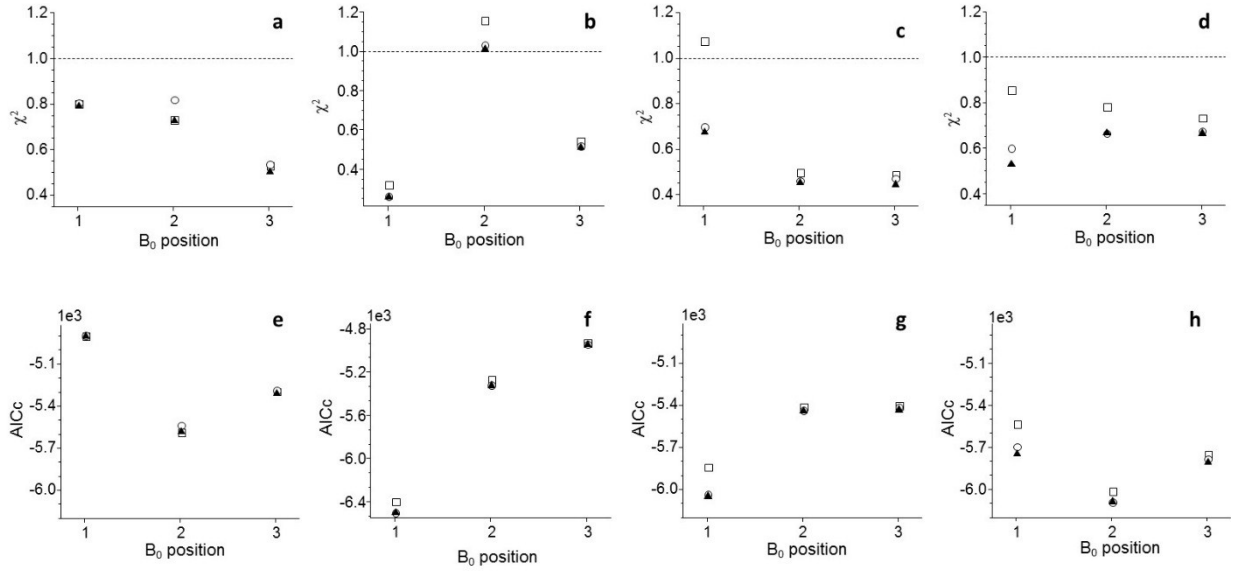

Figure S11: Goodness of fit comparison for DEER data fit to Gaussian models. (**a-d**) Reduced χ^2 values of G4 + CuTMpyP4, G6+ CuTMpyP4, G8+ CuTMpyP4 and G10 + CuTMpyP4, respectively. The horizontal dashed line indicates an ideal fit where the error is fully explained by the noise in the data. (**e-h**) The Akaike information criterion corrected (AICc) of G4 + CuTMpyP4, G6+ CuTMpyP4, G8+ CuTMpyP4 and G10 + CuTMpyP4, respectively. For all plots, unprocessed DEER data are modeled using either one Gaussian peak (open squares), two Gaussian peaks (open circles) or three Gaussian peaks (filled triangles) at the indicated field positions.

References

1. D. Akhmetzyanov, J. Plackmeyer, B. Endeward, V. Denysenkov and T. F. Prisner, *Physical Chemistry Chemical Physics*, 2015, **17**, 6760-6766.